Journal of Solid State Chemistry **163,** 253–258 (2002)
doi:10.1006/jssc.2001.9400, available online at http://www.idealibrary.com on IDEAL®

Low-Temperature Crystal Structure of S-camphor Solved from Powder Synchrotron X-ray Diffraction Data by Simulated Annealing

Michela Brunelli

ESRF, BP220, F-38043 Grenoble Cedex, France
E-mail: brunelli@esrf.fr

Andrew N. Fitch

ESRF, BP220, F-38043 Grenoble Cedex, France, and Department of Chemistry, Keele University, Staffordshire ST5 5BG, United Kingdom

and

Asiloé J. Mora

Departamento de Química, Facultad de Ciencias, Universidad de Los Andes, Mérida, Venezuela, and Department of Chemistry, Keele University, Staffordshire ST5 5BG, United Kingdom

Received July 10, 2001; in revised form September 5, 2001; accepted September 14, 2001

The ordered, low-temperature crystal structure of the pure enantiomer of camphor ($C_{10}H_{16}O$) has been solved from high-resolution powder synchrotron X-ray diffraction data. The structure is orthorhombic, space group $P2_12_12_1$, $Z = 8$, with $a = 8.9277(2)$ Å, $b = 27.0359(5)$ Å, and $c = 7.3814(1)$ Å at 100 K. The structure was solved by autoindexing of the pattern, space group determination, and then optimization of the positions and orientations of the two independent molecules in the unit cell by simulated annealing. The molecular structure obtained from the restrained Rietveld refinement shows reasonable agreement with that optimized from *ab initio* molecular orbital calculations. In the crystal structure, the molecules are aligned antiferroelectrically and weak C–H … O hydrogen bonds link together the independent molecules.

Key Words: **phase transitions; small ring systems; structure elucidation; X-ray diffraction.**

1. INTRODUCTION

The low-temperature behavior of solid camphor, (1,7,7-trimethyl-bicyclo[2.2.1]hepta-2-one, $C_{10}H_{16}O$), has been of considerable interest. Camphor is a simple chiral bicyclic organic molecule (Fig. 1), whose enantiomers are miscible in all proportions. The binary phase diagram of camphor was originally determined by Shäfer and Wagner (1). Below the melting point, irrespective of the composition, phase I has a cubic structure, which transforms on cooling to the hexagonal phase II which is stable at room temperature (2, 3). Phases I and II are orientationally-disordered, plastic phases, as are often found with globular molecules. The transition between the more-ordered, low-temperature phase III and phase II depends markedly on the composition. For the pure enantiomer the transition is at 244.19 K (4). For the 3:1 solid solution of enantiomers the minimum value near 190 K is reached. For the 1:1 racemic solid solution, RS-camphor, the transition occurs in a range of temperatures between 204 and 220 K depending on the thermal history (4).

There are other differences in behavior at the low-temperature transition depending on the composition. The NMR second moment has an abrupt decrease at the transition for the pure enantiomer, while it decreases almost linearly in RS-camphor (5). Dielectric studies (3, 5) also reveal distinct behavior for solutions with compositions near to the pure enantiomer or the racemate. The latter shows extensive pretransition effects. In the earlier work of Rossiter (6), different behavior for RS-camphor and the pure enantiomer was observed, and an increase of freedom of molecular rotation during the phase transition was deduced. Heat-capacity measurements (4) on R- and RS-camphor show that the latter exhibits an entropy relaxation process characteristic of a glass transition in the temperature range 70–100 K, and indicate excess entropy of $1.6 \pm 0.4\,\mathrm{J\,K^{-1}\,mol^{-1}}$ at 0 K. Equilibrium condition can be reached only by means of prolonged annealing. RS-camphor cooled

0022-4596/02 $35.00

normally therefore has residual disorder, whereas the pure enantiomer appears to be fully ordered. An early powder X-ray diffraction study (5) showed that the powder diffraction patterns of R-camphor, RS-camphor, and the 3:1 solution are identical at room temperature, but different at 77 K.

The disordered crystal structure of phase III of normally cooled RS-camphor was solved using powder synchrotron X-ray diffraction (7, 8). After determination of the unit cell from the peak positions, the arrangement of molecules was deduced by a combination of direct methods, which indicated the general location of the molecules in the cell, followed by a grid-search of molecular orientations. We have now solved the low-temperature structure of the pure enantiomer at 100 K and found it to be ordered, as expected from its physical properties.

2. EXPERIMENTAL

The powder diffraction pattern of S-camphor (Aldrich, 99%) was measured overnight with a wavelength of 0.6006(1) Å using the high-resolution powder diffraction beam line BM16 (9) at the ESRF, Grenoble. The sample was contained in a spinning 1.5-mm-diameter borosilicate glass capillary mounted on the axis of the diffractometer and cooled to 100 K by an Oxford Cryosystems Cryostream cold nitrogen blower mounted coaxially. The normalized diffraction profile used in the Rietveld analysis (3.5–40.0° 2θ) had 7301 points and contributions from 1632 Bragg peaks.

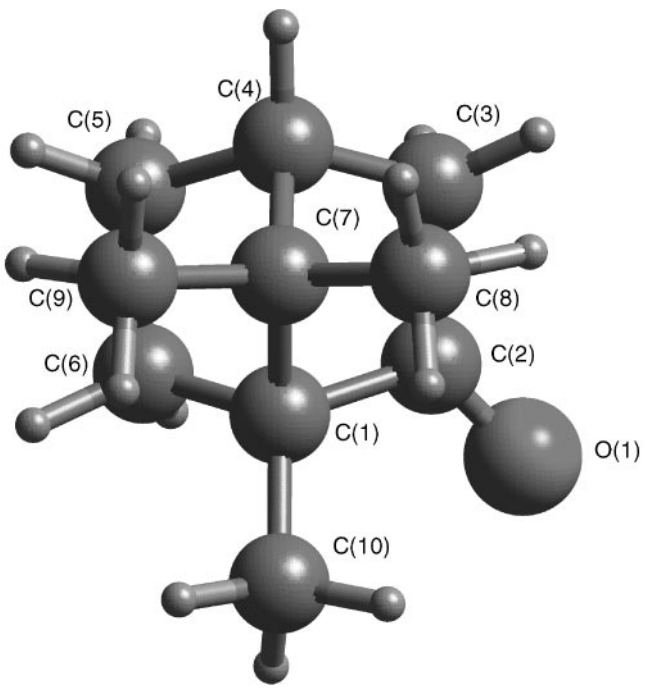

FIG. 1. Camphor and the labeling of the atoms.

TABLE 1

Final Parameters at 100 K for S-camphor ($C_{10}H_{16}O$, MWt, 152.24), after Rietveld Refinement in the Orthorhombic Space Group $P2_12_12_1$, $a = 8.9277(2)$ Å, $b = 27.0359(5)$ Å, $c = 7.3814(1)$ Å, $B_{overall} = 0.49(1)$ Å^2, $V = 1781.6(1)$ Å^3, $\rho = 1.135$ g/cm^3, $Z = 8$

atom	x	y	z
C(1)	0.475(1)	0.0999(3)	0.291(1)
C(2)	0.6414(9)	0.1136(2)	0.253(2)
C(3)	0.7346(7)	0.0661(3)	0.269(1)
C(4)	0.6099(9)	0.0282(2)	0.307(1)
C(5)	0.5533(8)	0.0361(3)	0.505(1)
C(6)	0.4735(9)	0.0880(3)	0.497(1)
C(7)	0.478(1)	0.0481(3)	0.199(1)
C(8)	0.5002(9)	0.0483(3)	−0.011(1)
C(9)	0.3247(6)	0.0197(3)	0.226(1)
C(10)	0.3584(8)	0.1375(3)	0.227(1)
O(1)	0.6834(6)	0.1552(2)	0.224(1)
H(1)	0.792(2)	0.0577(5)	0.144(2)
H(2)	0.812(1)	0.068(1)	0.381(2)
H(3)	0.639(1)	−0.0095(3)	0.275(2)
H(4)	0.474(1)	0.0076(3)	0.542(2)
H(5)	0.646(1)	0.0370(6)	0.600(1)
H(6)	0.360(1)	0.0854(6)	0.547(2)
H(7)	0.536(2)	0.1153(4)	0.572(1)
H(8)	0.488(6)	0.0111(5)	−0.062(2)
H(9)	0.418(4)	0.072(2)	−0.074(2)
H(10)	0.611(3)	0.062(2)	−0.044(2)
H(11)	0.380(4)	0.147(2)	0.0876(3)
H(12)	0.247(1)	0.122(1)	0.240(8)
H(13)	0.365(4)	0.170(1)	0.310(6)
H(14)	0.329(2)	−0.015(1)	0.155(6)
H(15)	0.306(3)	0.013(2)	0.369(2)
H(16)	0.234(1)	0.042(1)	0.173(6)
C(11)	0.4929(9)	0.3482(3)	0.231(1)
C(12)	0.525(1)	0.3651(3)	0.428(1)
C(13)	0.4999(9)	0.3173(3)	0.5360(8)
C(14)	0.4618(9)	0.2789(2)	0.389(1)
C(15)	0.2987(8)	0.2897(3)	0.324(1)
C(16)	0.3203(8)	0.3419(3)	0.233(1)
C(17)	0.5568(8)	0.2946(3)	0.229(1)
C(18)	0.7309(7)	0.2962(3)	0.248(1)
C(19)	0.515(1)	0.2692(3)	0.042(1)
C(20)	0.542(1)	0.3876(3)	0.0945(9)
O(2)	0.5565(7)	0.4058(2)	0.4828(9)
H(17)	0.601(2)	0.3069(5)	0.607(2)
H(18)	0.407(2)	0.3214(5)	0.629(2)
H(19)	0.480(1)	0.2410(1)	0.431(1)
H(20)	0.262(1)	0.2624(4)	0.227(2)
H(21)	0.222(1)	0.2920(7)	0.437(1)
H(22)	0.276(2)	0.3417(6)	0.097(2)
H(23)	0.268(1)	0.3706(4)	0.312(3)
H(24)	0.772(1)	0.2594(6)	0.275(8)
H(25)	0.780(1)	0.310(2)	0.124(4)
H(26)	0.761(1)	0.320(2)	0.358(6)
H(27)	0.661(1)	0.393(1)	0.106(6)
H(28)	0.514(7)	0.376(1)	−0.041(1)
H(29)	0.486(6)	0.4220(7)	0.125(6)
H(30)	0.535(7)	0.2298(4)	0.050(3)
H(31)	0.398(2)	0.276(2)	0.012(5)
H(32)	0.583(5)	0.285(1)	−0.065(2)

Note. R-factors: $R_{wp} = 8.4\%$, $R_I = 2.5\%$, $\chi^2 = 37$.

The pattern was indexed with a figure of merit (10) M_{20} of 40 using the program Fzon (11) from the positions of 20 low-angle reflections. The density of camphor indicates that there are eight molecules in the orthorhombic cell found. The systematic absences suggested the space group $P2_12_12_1$, hence two distinct molecules in the asymmetric unit. Attempts to solve the structure by the direct-methods package EXPO (12) to locate the 22 nonhydrogen atoms constituting the two independent molecules were unsuccessful.

Attempts were therefore made to solve the structure by a direct-space method. Direct-space methods move molecules around the unit cell, varying position, orientation and, where appropriate, torsion angles, and attempt to minimize the discrepancy between the observed and calculated diffraction data under the control of a global-minimization procedure. Bond lengths and angles can also be varied if they are not adequately known in advance. The effectiveness of these methods is illustrated by a number of recent publications, which use techniques such as Monte-Carlo (13–16), simulated annealing (17–19), or genetic algorithms (20–24). Complex structure with more than one fragment in the unit cell, or with multiple torsion angles (up to 15) have been solved from powder data (19, 24–27).

For S-camphor the program PowderSolve (28) was applied with its default parameters to control the simulated annealing. Direct-space methods require an accurate structure for the molecule. We used the molecular structure used in (7) derived from the single-crystal X-ray diffraction study of the clathrate formed between camphor and deoxycholic acid (29). For S-camphor, there are two independent

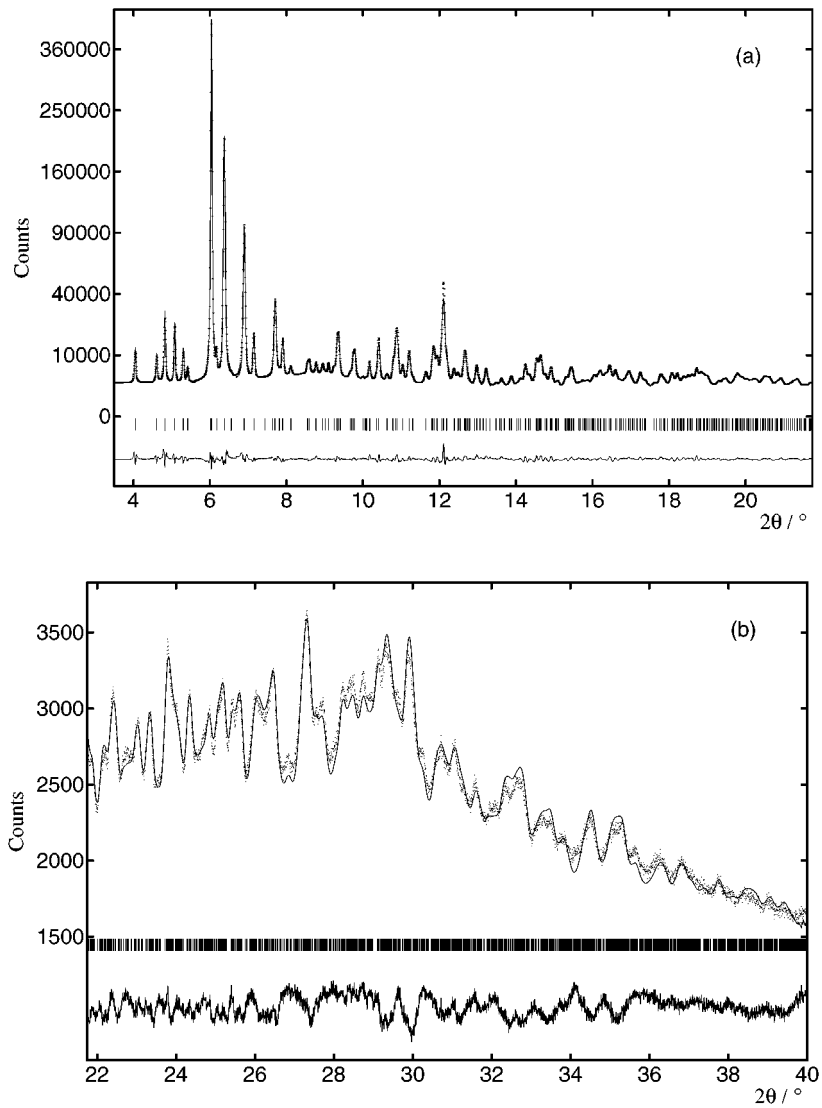

FIG. 2. Observed (·), calculated (—), and difference plot of the Rietveld refinement of the low-temperature phase of S-camphor in the low (a) (y axis in square-root scale) and high (b) angle range; reflection positions are shown as vertical lines.

molecules requiring, therefore, six degrees of translational freedom and six degrees of orientational freedom to describe the structure. The structure was solved with a 10-day run on a Silicon Graphics O2 machine, performed in two distinct steps encompassing 100 million and then 10 million cycles of simulated annealing. In the first run, all six translational and six rotational degrees of freedom of the two molecules were allowed to vary. However, it was clear that the best solution found was not correct. Although the fit to the low-angle data looked very promising, the high-angle agreement was poor. In the next stage, only the six orientations were allowed to vary. The molecules were able simply to reorient about the best position found in the first minimization stage. This improved convincingly the match between the calculated and the observed diffraction patterns, and it was clear that the correct solution had been found.

A Rietveld (30) refinement of the structure was performed with the program WinMProf (31), in which the peaks were described by a pseudo-Voigt peak shape function incorporating anisotropic broadening (32). Low angle asymmetry was corrected with the model of Baldinozzi and Bérar (33). Atomic positions were refined with C–H distances restrained to 1.080 Å (weighted 0.001 Å) and tetrahedral angles to 109.5° (weighted 0.5°). Furthermore, corresponding C–C and C–O distances in the two independent molecules were restrained to have the *same* unspecified values with a weighting of 0.001 Å. An overall isotropic temperature factor was refined. The fit is shown in Fig. 2, with *R*-factors and refined atomic parameters in Table 1.

3. DISCUSSION

The two-step simulated annealing procedure was effective because the agreement between the observed and calculated diffraction profiles is significantly more sensitive to the position of a molecule in the cell than to its orientation (Fig. 3). This is presumably due to the globular nature of the camphor molecule. Hence, if the minimization procedure fails to find the global minimum, it is nevertheless more likely to find a configuration that has a molecule in the correct position with the incorrect orientation, rather than the inverse. This two-step approach reflects to some extent the case of the racemic solid solution RS-camphor (7), in which the correct orientation for the camphor molecule was obtained once the overall position had been established by direct methods. In a similar vein, to position a single molecule in the unit cell via a Patterson search method, the search can be split into two three-dimensional searches, a rotational search followed by a translational search (34–36).

In Table 2 bond lengths and angles in the camphor molecule are reported, compared with the values obtained

TABLE 2
Average Bond Lengths and Angles of S-camphor at 100K and Comparison with the Results from an *ab-initio* Molecular Orbital Calculation (37)

Bond lengths (Å)	Powder diffraction	6-31 + G(d) MO calculation
C(1)–C(2)	1.55(2)	1.528
C(1)–C(6)	1.55(2)	1.558
C(1)–C(7)	1.56(1)	1.562
C(1)–C(10)	1.53(1)	1.519
C(2)–C(3)	1.53(1)	1.531
C(2)–O(1)	1.20(1)	1.185
C(3)–C(4)	1.54(1)	1.540
C(4)–C(5)	1.56(1)	1.542
C(4)–C(7)	1.52(1)	1.557
C(5)–C(6)	1.57(1)	1.556
C(7)–C(8)	1.56(1)	1.540
C(7)–C(9)	1.58(1)	1.536
Angles (°)		
C(2)–C(1)–C(6)	103(2)	103.3
C(2)–C(1)–C(7)	100(1)	100.4
C(2)–C(1)–C(10)	113(1)	114.0
C(6)–C(1)–C(7)	104(1)	102.2
C(6)–C(1)–C(10)	114(2)	115.0
C(7)–C(1)–C(10)	120(2)	119.8
C(1)–C(2)–C(3)	105(1)	106.6
C(1)–C(2)–O(1)	126(2)	126.9
C(3)–C(2)–O(1)	129(2)	126.5
C(2)–C(3)–C(4)	102(1)	101.7
C(3)–C(4)–C(5)	108(1)	106.5
C(3)–C(4)–C(7)	103(1)	102.6
C(5)–C(4)–C(7)	102(1)	102.8
C(4)–C(5)–C(6)	102(1)	102.7
C(1)–C(6)–C(5)	103(1)	104.3
C(1)–C(7)–C(4)	94(1)	93.9
C(1)–C(7)–C(8)	113(1)	113.6
C(1)–C(7)–C(9)	110(2)	114.7
C(4)–C(7)–C(8)	117(2)	113.9
C(4)–C(7)–C(9)	115(1)	113.7
C(8)–C(7)–C(9)	106(1)	107.0

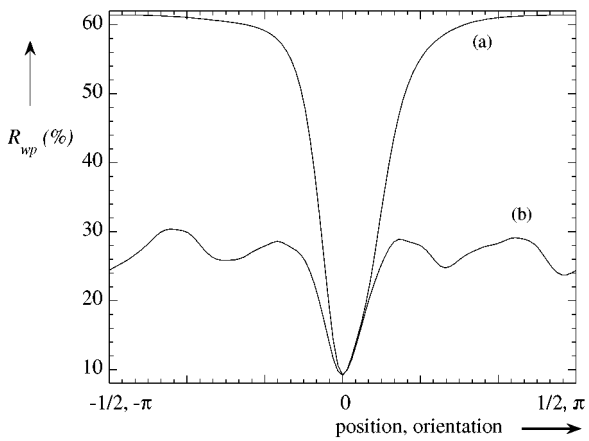

FIG. 3. Typical variation of R_{wp} in PowderSolve as a molecule is (a) translated by one lattice unit or (b) rotated by 2π about the global minimum.

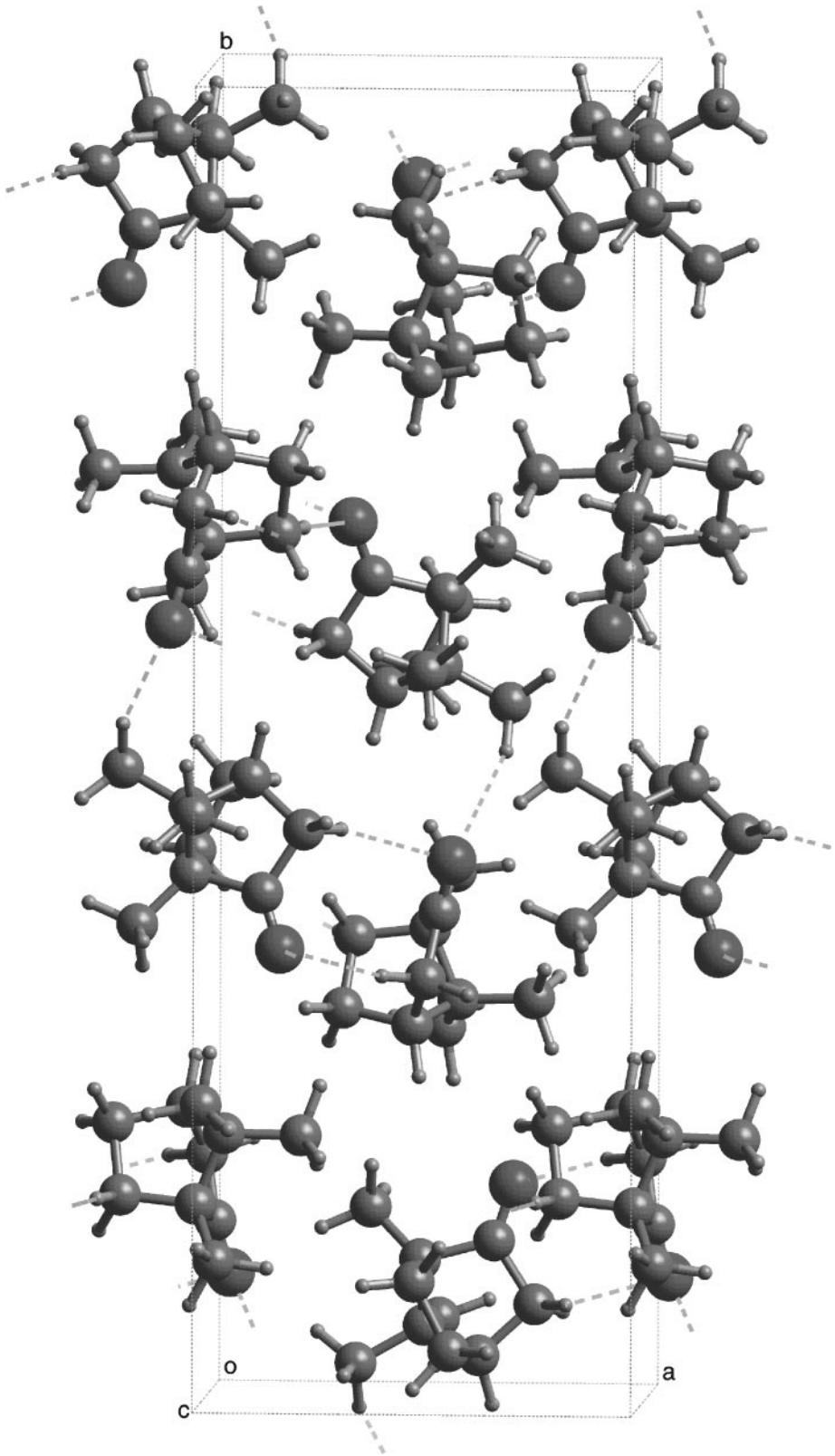

FIG. 4. View of the low-temperature structure of S-camphor. The four shortest C–H ··· O hydrogen bonds are shown, C(3) ··· O(2), C(9) ··· O(2), C(13) ··· O(1), and C(16) ··· O(1). The molecular dipole moments are aligned antiferroelectrically about the *b* direction.

TABLE 3
Possible (38) C–H ··· O Hydrogen-Bond Distances and Angles

Hydrogen bond (Å)	C ··· O distance (Å)	H ··· O distance (Å)	C–H ··· O angle (°)
C(13)–H(18) ··· O(1)	3.42(1)	2.36	165.4
C(15)–H(21) ··· O(1)	3.80(1)	2.90	140.2
C(16)–H(22) ··· O(1)	3.59(1)	2.51	176.9
C(19)–H(30) ··· O(1)	3.68(1)	2.73	146.5
C(3)–H(2) ··· O(2)	3.49(1)	2.50	152.0
C(6)–H(6) ··· O(2)	3.73(1)	2.73	153.9
C(9)–H(14) ··· O(2)	3.60(1)	2.58	158.2
C(10)–H(12) ··· O(2)	3.64(1)	2.77	137.2

from an *ab initio* molecular-orbital calculation using Gaussian 94 (37) with a 6-31 + G(d) basis set. The agreement between the two sets of values is generally quite good, but there are some distances and angles that appear to be inaccurately determined from the powder-diffraction data. This indicates that despite the high resolution and quality of patterns now available from a third-generation synchrotron-radiation source, the accuracy of refined structures is still limited, presumably because of the problems caused by peak overlap in the powder pattern.

The crystal structure of S-camphor is larger and more complex than that of RS-camphor, and is ordered, as previously indicated by its physical properties. Nevertheless, both structures have antiferroelectric ordering of the dipole moments (calculated to be 3.30 D by Gaussian 94 (37)). The eight molecules of camphor placed in the unit cell are illustrated in Fig. 4. This is a rare chance to observe the interactions of the camphor molecule in an ordered crystal structure. There are several C–H ··· O hydrogen bonds forming a network and stabilizing the packing between the two crystallographically distinct molecules (Table 3).

Further work is required to investigate compositions around the three-to-one ratio, at which the lowest temperature for the transition from phase III to phase II is attained. This may represent a different crystal structure, or a transitional stage from the fully ordered enantiomer to the fourfold-disordered structure of the racemic solid solution.

ACKNOWLEDGMENTS

We thank the European Synchrotron Radiation Facility, Grenoble, (ESRF), for providing beam time on the high-resolution powder diffraction beam line BM16.

REFERENCES

1. K. L. Shäfer and U. Wagner, *Z. Elektrochem.* **62,** 328–335 (1958).
2. C. C. Mjojo, *J. Chem. Soc. Faraday Trans.* 2 **75,** 692–703 (1979).
3. C. C. Mjojo and H. K. Welsh, *J. Chem. Soc. Faraday Trans.* **88,** 2909–2913 (1992).
4. T. Nagumo, T. Matsuo, and H. Suga, *Thermochim. Acta* **139,** 121–132 (1989).
5. J. E. Anderson and W. P. Slichter, *J. Chem. Phys.* **41,** 1922–1928 (1964).
6. V. Rossiter, *J. Phys. C* **5,** 1969–1975 (1972).
7. A. J. Mora and A. N. Fitch, *J. Solid State Chem.* **134,** 211–214 (1997), doi: 10.1006/jssc.1997.7648.
8. A. J. Mora and A. N. Fitch, *Mater. Sci. Forum* **228,** 863–868 (1996).
9. A. N. Fitch, *Mater. Sci. Forum* **228–231,** 219–222 (1996).
10. P. M. De Wolff, *J. Appl. Crystallogr.* **1,** 108–113 (1968).
11. J. W. Visser, *J. Appl. Crystallogr.* **2,** 89–95 (1969).
12. A. Altomare, M. C. Burla, M. Camalli, B. Carrozzini, G. L. Cascarano, C. Giacovazzo, A. Guagliardi, A. G. G. Moliterni, G. Polidori, and R. Rizzi, *J. Appl. Crystallogr.* **32,** 339–340 (1999).
13. Y. G. Andreev, P. Lightfoot, and P. G. Bruce, *J. Appl. Crystallogr.* **30,** 294–305 (1997).
14. M. Tremayne, B. M. Kariuki, and K. D. M. Harris, *J. Appl. Crystallogr.* **29,** 211–214 (1996).
15. M. Tremayne, B. M. Kariuki, and K. D. M. Harris, *Angew. Chem. Int. Ed. Engl.* **36,** 770–772 (1997).
16. Y. G. Andreev, P. Lightfoot, and P. G. Bruce, *Chem. Commun.* 2169–2170 (1996).
17. Y. G. Andreev, and P. G. Bruce, *J. Chem. Soc. Dalton Trans.* 4071–4080 (1998).
18. Y. G. Andreev, G. S. MacGlashan, and P. G. Bruce, *Phys. Rev. B* **55,** 12011–12017 (1997).
19. W. I. F. David, K. Shankland, and N. Shankland, *Chem. Commun.* 931–932 (1998).
20. K. Shankland, W. I. F. David, and T. Csoka, *Z. Kristallogr.* **212,** 550–552 (1997).
21. K. D. M. Harris, R. L. Johnston, and B. M. Kariuki, *Acta Crystallogr. A* **54,** 632–645 (1998).
22. E. Tedesco, G. W. Turner, K. D. M. Harris, R. L. Johnston, and B. M. Kariuki, *Angew. Chem. Int. Ed. Engl.* **39,** 4488–4491 (2000).
23. K. Shankland, W. I. F. David, T. Csoka, and L. McBride, *Int. J. Pharmaceut.* **165,** 117–126 (1998).
24. B. M. Kariuki, P. Calcagno, K. D. M. Harris, D. Philp, and R. L. Johnston, *Angew. Chem. Int. Ed. Engl.* **38,** 831–835 (1999).
25. G. S. MacGlashan, Y. G. Andreev, and P. G. Bruce, *Nature* **398,** 792–794 (1999).
26. M. J. Tremayne and C. Glidewell, *Chem. Commun.* 2425–2426 (2000).
27. A. M. T. Bell, J. N. B. Smith, J. P. Attfield, J. M. Rawson, K. Shankland, and W. I. F. David, *New J. Chem.* **23,** 565–568 (1999).
28. G. E. Engel, S. Wilke, O. König, K. D. M. Harris, and F. J. J. Leusen, *J. Appl. Crystallogr.* **32,** 1169–1179 (1999).
29. S. Candeloro De Sanctis, V. M. Coiro, F. Mazza, and G. Pochetti, *Acta Crystallogr. B* **51,** 81–89 (1995).
30. H. M. Rietveld, *J. Appl. Crystallogr.* **2,** 65–71 (1969).
31. A. Jouanneaux, CPD *Newsletter* **21,** 13 (1999).
32. P. W. Stephens, *J. Appl. Crystallogr.* **32,** 281–289 (1999).
33. J.-F. Bérar and G. Baldinozzi, *J. Appl.* **26,** 128–129 (1993).
34. J. Cirujeda, L. E. Ochando, J. M. Amigó, C. Rovira, J. Rius, and J. Veciana, *Angew. Chem. Int. Ed. Engl.* **34,** 55–57 (1995).
35. J. Rius and C. Miravitlles, *J. Appl. Crystallogr.* **21,** 224–227 (1988).
36. J. Rius and C. Miravitlles, *J. Appl. Crystallogr.* **20,** 260–261 (1987).
37. M. J. Frisch, G. W. Trucks, H. B. Schlegel, P. M. W. Gill, B. G. Johnson, M. A. Robb, J. R. Cheeseman, T. Keith, G. A. Petersson, J. A. Montgomer, K. Raghavachari, M. A. Al-Laham, V. G. Zakrzewski, J. V. Ortiz, J. B. Foresman, J. Cioslowski, B. B. Stefanov, A. Nanayakkara, M. Challacombe, C. Y. Peng, P. Y. Ayala, W. Chen, M. W. Wong, J. L. Andres, E. S. Replogle, R. Gomperts, R. L. Martin, D. J. Fox, J. S. Binkley, D. J. Defrees, J. Baker, J. P. Stewart, M. Head-Gordon, C. Gonzalez, and J. A. Pople, Gaussian, Inc., Pittsburgh PA, 1995.
38. G. R. Desiraju, *Acc. Chem. Res.* **29,** 441–449 (1996).